# Hydrogen-Passivated Graphene Antidot Structures for Thermoelectric Applications

Hossein Karamitaheri[1,2], Mahdi Pourfath[2], Rahim Faez[1], Hans Kosina[2]
[1]School of Electrical Engineering, Sharif University of Technology, Tehran, Iran
[2]Technische Universität Wien, Institute for Microelectronics
Gußhausstraße 27–29/E360, A-1040 Wien, Austria
email: pourfath@iue.tuwien.ac.at

**Abstract**

In this work, we present a theoretical investigation of the thermal conductivity of hydrogen-passivated graphene antidot lattices. Using a fourth nearest-neighbor force constant method, we evaluate the phonon dispersion of hydrogen-passivated graphene antidot lattices with circular, hexagonal, rectangular and triangular shapes. Ballistic transport models are used to evaluate the thermal conductivity. The calculations indicate that the thermal conductivity of hydrogen-passivated graphene antidot lattices can be one fourth of that of a pristine graphene sheet. This reduction is stronger for right-triangular and iso-triangular antidots among others, all with the same area, due to longer boundaries and the smallest distance between the neighboring dots.

## 1. Introduction

Today, thermoelectric devices can be used in a very wide range of applications including energy harvesting, aerospace and military applications. The thermoelectric figure of merit is defined as:

$$ZT = \frac{S^2 \sigma T}{(K_{\rm el} + K_{\rm ph})} \qquad (1)$$

where $S$, $\sigma$, $T$, $K_{\rm el}$ and $K_{\rm ph}$ are the Seebeck coefficient, the electrical conductivity, temperature, and the electrical and lattice contributions to the thermal conductivity, respectively [1]. The numerator of $Z$ is called power factor. The figure of merit determines the efficiency of a thermoelectric device and can be improved by increasing the power factor and decreasing the thermal conductivity. Hence, thermoelectric materials must simultaneously have a high Seebeck coefficient, a high electrical conductivity and a low thermal conductivity.

Bismuth and its alloys that are commonly used in thermoelectric applications [2], suffer from high cost, as the use of heavy metals in large scale applications is limited. On the contrary, bulk silicon has a very low $ZT \approx 0.01$ [3], because of its high thermal conductivity. While each property of $ZT$ can individually be changed by several orders of magnitude, the interdependence and coupling between these properties have made it extremely difficult to increase $ZT > 1$. In recent years many studies have been conducted for employing new materials and technologies to improve $ZT$. Progress in nanomaterials synthesis has allowed the realization of low-dimensional thermoelectric device structures such as one-dimensional nanowires, thin films, and two-dimensional superlattices [4–6]. However, the recent breakthroughs in materials with $ZT > 1$ have mainly benefited from reduced phonon thermal conductivity [6, 7].

Graphene, a recently discovered form of carbon, has received much attention over past few years due to its excellent electrical, optical, and thermal properties [8]. The electrical conductivity of graphene is as high as that of cooper [9] and it has a giant Seebeck coefficient [10]. In addition, a large scale method to produce graphene sheets has been reported [11]. These factors render graphene as a candidate for future thermoelectric applications.

However, the ability of graphene to conduct heat is an order of magnitude higher than that of copper [12]. Therefore, it is necessary to reduce its thermal conductivity. The high thermal conductivity of graphene is mostly due to the lattice contribution, whereas the electronic contribution to the thermal conduction can be ignored [12, 13]. Therefore, by proper engineering of phonon transport it is possible to reduce the total thermal conductivity without significant reduction of the electrical conductivity and the power factor.

Recently many theoretical studies have been performed on the thermal conductivity of graphene-based structures. It has been shown that boundaries and edge roughness can strongly influence the thermal conductivity [14]. Furthermore, it has been recently shown that the thermal conductivity of graphene nanoribbons can be reduced by hydrogen-passivation of the edges [15].

In this work we investigate the thermal conductivity of graphene-based antidot lattices [16]. We show that by introducing hydrogen-passivated (H-passivated) dots in the graphene sheet (Fig. 1) the thermal conductivities of graphene antidot lattices (GALs) decrease and the respective $ZT$ values increase.

*978-1-4577-0106-1/11/$26.00 ©2011 IEEE*



*2011 12th. Int. Conf. on Thermal, Mechanical and Multiphysics Simulation and Experiments in Microelectronics and Microsystems, EuroSimE 2011*

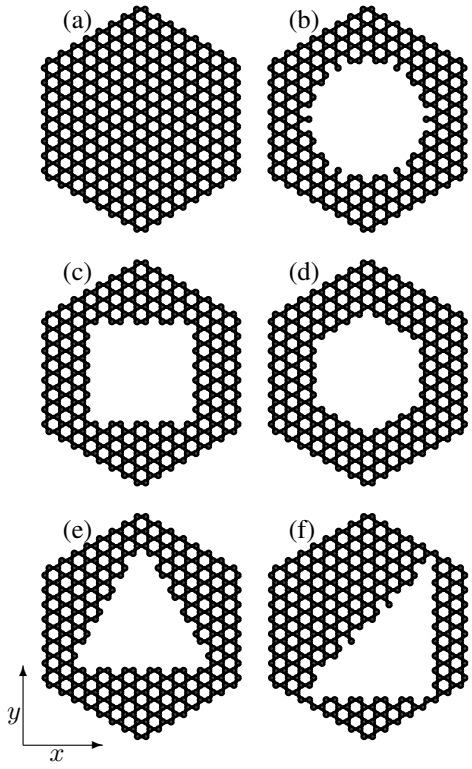


Figure 1: The geometry structures of different H-passivated GALs. (a)-(f) indicate a pristine graphene, Circ(8, 108), Rect(8, 104), Hex(8, 96), IsoTri(8, 90), and RTri(8, 95), respectively.

Table I: Number of edge carbon atoms in a unit cell of different GALs that have been passivated by hydrogen atoms. Atomic mass of these carbon atoms are considered to be 13 amu.

| **Structure** | **Number of boundary atoms** |
|---|---|
| Circ$(8, 108)$ | 30 |
| Rect$(8, 104)$ | 28 |
| Hex$(8, 96)$ | 24 |
| IsoTri$(8, 90)$ | 30 |
| RTri$(8, 95)$ | 33 |

Table II: Elements of the force constant tensor up to fourth nearest-neighbors [17]. $\Phi_r$, $\Phi_{ti}$ and $\Phi_{to}$ are the radial, in-plane transverse, and out-of-plane transverse components of the force constant tensor, respectively. The unit is N/m.

| **NN** | $\Phi_r$ | $\Phi_{ti}$ | $\Phi_{to}$ |
|---|---|---|---|
| 1 | 365.0 | 245.0 | 98.2 |
| 2 | 88.0 | -32.3 | -4.0 |
| 3 | 30.0 | -52.5 | 1.5 |
| 4 | -19.2 | 22.9 | -5.8 |

## 2. Structures

We investigate GALs with various dot shapes that are passivated with hydrogen atoms. In Fig.1 Circ, Rect, Hex, IsoTri, and RTri indicate a circular, rectangular, hexagonal, iso-triangular, and right-triangular dot in the hexagonal unit cell, respectively. The unit cell of GALs is specified by a pair of parameters $(L, N)$, where $L$ is the side length of the hexagon in terms of the graphene lattice constant $a = 2.46\mathring{A}$ and $N$ is the number of carbon atoms that are removed from the pristine graphene supercell. Fig.1-b shows a circular GAL that is created by removing 108 carbon atoms from a hexagonal pristine supercell with a side length of $L = 8$. It is therefore, represented by Circ(10,108). The number of edge carbon atoms in a unit cell of different GALs is also given in Table I. As we will show later the number of carbon atoms at the boundary plays an important role on the thermal properties of the structure.

## 3. Calculation Methods

We performed a numerical study of the thermal properties of H-passivated GALs. The phonon dispersion is evaluated using a fourth nearest-neighbor force constant method. Using the dispersion, the ballistic transmission that is equal to the density of modes $M(E)$ is evaluated [18]. Finally, the thermal conductance is calculated by employing ballistic transport models.

### 3.1. Phonon Dispersion

To evaluate the Phonon dispersion of H-passivated GALs, a fourth nearest-neighbor force constant method is employed. The dynamical matrix defined by

$$D^{ij}(k) = \left( \sum_l K^{il} - M_i \omega^2(k) I \right) \delta_{ij} - \sum_l K^{il} e^{i\mathbf{k}\cdot\Delta\mathbf{R}_{il}} \quad (2)$$

where $M_i$ is the atomic mass of the $i$th atoms, $\Delta\mathbf{R}_{ij} = \mathbf{R}_i - \mathbf{R}_j$ is the distance between the $i$th atom and the $j$th atom, and $K^{ij}$ is a $3 \times 3$ force constant tensor with values given in Table II [17]. The phonon thermal conductivity is dominated by low frequency phonons. Therefore, high frequency motion of hydrogen atoms can be neglected by considering a higher atomic mass for edge carbon atoms [15]. Therefore, the atomic mass of edge carbon atoms are assumed to be 13 amu per atom, which is equal to the sum of the atomic mass of a hydrogen and a carbon atom.

### 3.2. Thermal Conductivity

The lattice contribution to the thermal conductance can be evaluated from the phonon transmission probability $\overline{T}_{\rm ph}$ [19] as:

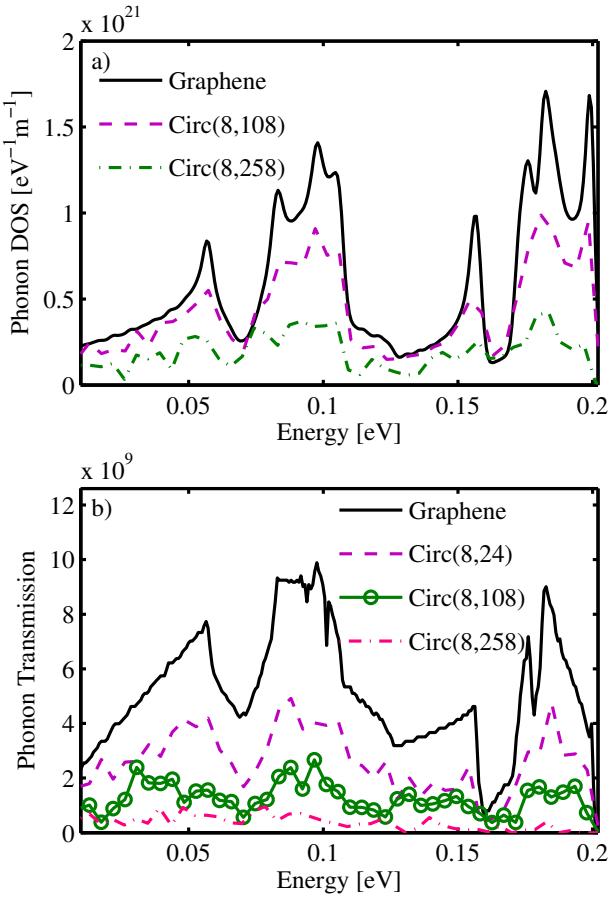


Figure 2: Comparison between (a) phonon density of states and (b) transmission probability of pristine graphene and circular H-passivated GALs with different dot areas.

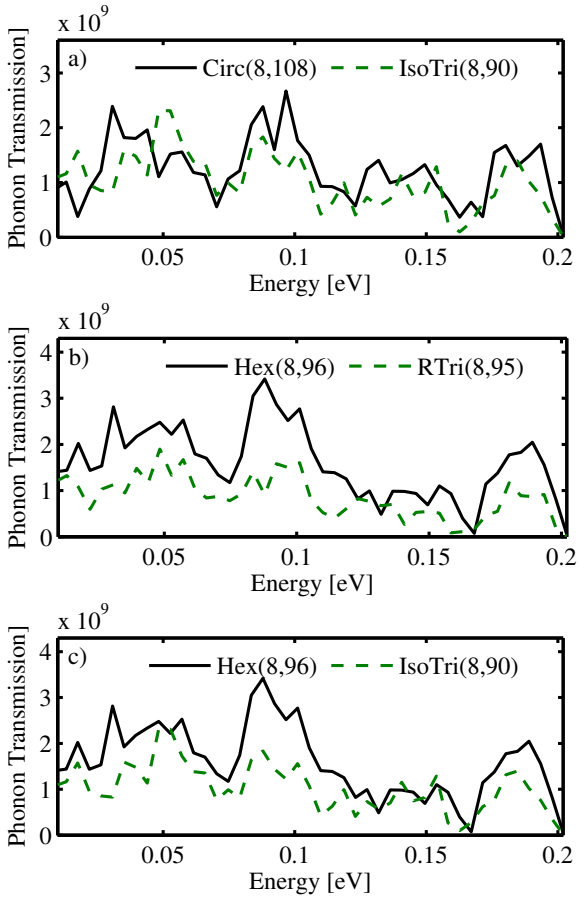


Figure 3: Comparison between the transmission probability of (a) Circ(8,10) and IsoTri(8,90), (b) Hex(8,96) and RTri(8,95), and (c) Hex(8,96) and IsoTri(8,90).

$$K_{\mathrm{ph}} = \frac{1}{h}\int_0^{+\infty} \overline{T}_{\mathrm{ph}}(\omega)\hbar\omega\left(\frac{\partial n(\omega)}{\partial T}\right) d(\hbar\omega) \qquad (3)$$

where $\hbar$ is the reduced Planck constant and $n(\omega)$ denotes the Bose-Einstein distribution function. In the ballistic regime, the transmission coefficient of each phonon mode is assumed to be one. Therefore, the transmission probability can be extracted from the density of modes [11, 18].

## 4. Results and Discussion

In the first step, we compare the thermal conductivity of circular GALs with $L = 8$ and different radii, including Circ(8,24), Circ(8,108) and Circ(8,258). The phonon density of states (DOS) and phonon transmission probability of these GALs are shown in Fig. 2. By increasing the size of the dot, the phonon DOS, the phonon transmission probability, and the thermal conductivity are significantly reduced (see Table III).

By increasing the radius, both the area and the circumference of dot are increased. To investigate the effect of circumference, we compare GALs with nearly the same area and different shapes, including Circ(8,108), Rect(8,104), Hex(8,96), IsoTri(8,90) and RTri(8,95). Among them, triangular GALs have the highest number of edge carbon atoms and Circ(8,108) has the largest dot size, and it has also a high number of edge atoms. In Fig. 3 the phonon transmission probabilities of Circ(8,108), Hex(8,96), IsoTri(8,90) and RTri(8,95) are compared. Although the dot size in Circ(8,108) is 15% larger than that of a IsoTri(8,90), the transmission probabilities of these GALs are quite similar (see Fig. 3-a). On the other hand, the transmission probabilities of IsoTri(8,90) and RTri(8,95) are significantly lower than that of Hex(8,96) (see Fig. 3-a and Fig. 3-b).

The normalized thermal conductivity of different H-passivated GALs with respect to graphene lattice thermal conductivity are summarized in Table III. Triangular GALs have the minimum thermal conductivity, although they have the minimum area of all dot shapes. This behavior can be explained by considering the fact that triangular dots have the highest circumference of all dots with the same area. This indicates that circumference of the dot has a stronger effect on thermal conductivity rather than its area.

Table III: The comparison of the thermal conductivities of different GALs. The results are normalized to the thermal conductivity of a pristine graphene.

| Structure | Normalized thermal conductance |
|---|---|
| Pristine Graphene | 1 |
| Circ$(8, 24)$ | 0.5527 |
| Circ$(8, 108)$ | 0.2618 |
| Circ$(8, 258)$ | 0.1016 |
| Rect$(8, 104)$ | 0.3054 |
| Hex$(8, 96)$ | 0.3817 |
| IsoTri$(8, 90)$ | 0.2402 |
| RTri$(8, 95)$ | 0.2101 |

## 5. Conclusion

We numerically analyzed the the role of the dot size, the circumference of the dots, and the distance between dots on the thermal properties of H-passivated GALs. We show that by appropriate selection of the geometrical parameters one can significantly reduce the thermal conductivity of graphene antidot lattices and improve their thermoelectric figure of merit. This helps us to design and improve the efficiency of graphene based thermoelectric devices for future energy harvesting and other thermoelectric applications.


## Acknowledgments

This work, as part of the ESF EUROCORES program EuroGRAPHENE, was partly supported by funds from FWF, contract I420-N16.


## References


[1] G.S. Nolas, J. Sharp, and H.J. Goldsmid, *Thermoelectrics: Basic Principles and New Materials Developments*, Springer, 2001.

[2] H.J. Goldsmid, *Introduction to Thermoelectricity*, chapter Review of Thermoelectric Materials, Springer, 2010.

[3] L. Weber and E. Gmelin, "Transport Properties of Silicon," *Appl. Phys. A*, vol. 53, pp. 136–140, 1991.

[4] A. I. Hochbaum, R. Chen, R. D. Delgado, W. Liang, E. C. Garnett, M. Najarian, A. Majumdar, and P. Yang, "Enhanced Thermoelectric Performance of Rough Silicon Nanowires," *Nature (London)*, vol. 451, no. 7175, pp. 163–167, 2008.

[5] A.I. Boukai, Y. Bunimovich, J. Tahir-Kheli, J.-K. Yu, W.A. Goddard, and J.R. Heath, "Silicon Nanowires as Efficient Thermoelectric Materials," *Nature (London)*, vol. 451, pp. 168–171, 2008.

[6] R Venkatasubramanian, E Siivola, T Colpitts, and B O'Quinn, "Thin-film Thermoelectric Devices with High Room-Temperature Figures of Merit.," *Nature*, vol. 413, no. 6856, pp. 597–602, 2001.

[7] T C Harman, P J Taylor, M P Walsh, and B E LaForge, "Quantum Dot Superlattice Thermoelectric Materials and Devices.," *Science*, vol. 297, no. 5590, pp. 2229–2232, 2002.

[8] K.S. Novoselov, A.K. Geim, S.V. Morozov, D. Jiang, Y. Zhang, S.V. Dubonos, and A.A. Firsov, "Electric Field Effect in Atomically Thin Carbon Films," *Science*, vol. 306, no. 5696, pp. 666–669, 2004.

[9] J.-H. Chen, C. Jang, S. Xiao, M. Ishighami, and M.S. Fuhrer, "Intrinsic and Extrinsic Performance Limits of Graphene Devices on $SiO_2$," *Nature Nanotech.*, vol. 3, no. 4, pp. 206–209, 2008.

[10] D. Dragoman and M. Dragoman, "Giant Thermoelectric Effect in Graphene," *Appl. Phys. Lett.*, vol. 91, pp. 203116, 2007.

[11] K.S. Kim, Y. Zhao, H. Jang, S.Y. Lee, J.M. Kim, K.S. Kim, J.-H. Ahn, P. Kim, J.-Y. Choi, and B.H. Hong, "Large-Scale Pattern Growth of Graphene Films for Stretchable Transparent Electrodes," *Nature (London)*, vol. 457, no. 7230, pp. 706–710, 2009.

[12] A. A. Balandin, S. Ghosh, W. Bao, I. Calizo, D. Teweldebrhan, F. Miao, and C. N. Lau, "Superior Thermal Conductivity of Single-Layer Graphene," *Nano Lett.*, vol. 8, no. 3, pp. 902–907, 2008.

[13] J. Hone, M. Whitney, C. Piskoti, and A. Zettl, "Thermal Conductivity of Single-Walled Carbon Nanotubes," *Phys. Rev. B*, vol. 59, pp. R2514–R2516, 1999.

[14] H. Sevincli and G. Cuniberti, "Enhanced Thermoelectric Figure of Merit in Edge-Disordered Zigzag Graphene Nanoribbons," *Phys. Rev. B*, vol. 81, pp. 113401, 2010.

[15] W.J. Evans, L. Hu, and P. Keblinski, "Thermal Conductivity of Graphene Ribbons from Equilibrium Molecular Dynamics: Effect of Ribbon Width, Edge Roughness, and Hydrogen Termination," *Appl. Phys. Lett.*, vol. 96, pp. 203112, 2010.

[16] J. Bai, X. Zhong, S. Jiang, Y. Huang, and X. Duan, "Graphene Nanomesh," *Nature Nanotech.*, vol. 5, pp. 190–194, 2010.

[17] R. Saito, T. Takeya, T. Kimura, G. Dresselhaus, and M. S. Dresselhaus, "Raman Intensity of Single-Wall Carbon Nanotubes ," *Phys. Rev. B*, vol. 57, no. 7, pp. 4145–4153, 1998.

[18] S. Datta, *Quantum Transport: From Atoms to Transistors*, Cambridge University Press, Cambridge, 2005.

[19] Y. Ouyang and J. Guo, "A Theoretical Study on Thermoelectric Properties of Graphene Nanoribbons," *Appl. Phys. Lett.*, vol. 94, pp. 263107 (3pp), 2009.